Energy Conversion and Management 231 (2021) 113835

Contents lists available at ScienceDirect

Energy Conversion and Management

journal homepage: www.elsevier.com/locate/enconman

Multi-objective optimization of hydrogen liquefaction process integrated with liquefied natural gas system

Ju-Eon Bae [a], Supaporn Wilailak [b], Jae-Hyeon Yang [a], Dong-Yeol Yun [a], Umer Zahid [c,*], Chul-Jin Lee [a,b,*]

[a] School of Chemical Engineering and Materials Science, Chung-Ang University, 84, Heukseok-ro, Dongjak-gu, Seoul, Republic of Korea
[b] Department of Intelligent Energy and Industry, Chung-Ang University, 84, Heukseok-ro, Dongjak-gu, Seoul, Republic of Korea
[c] Chemical Engineering Department, King Fahd University of Petroleum and Minerals, Dhahran, Saudi Arabia

ARTICLE INFO

Keywords:
Hydrogen Liquefaction
Genetic Algorithm
Multi-objective Optimization

ABSTRACT

Liquid hydrogen is gaining increasing attention owing to its high energy density as 10.1 MJ/L compared to gaseous hydrogen as 5.6 MJ/L at 700 bar. However, the energy required for its cryogenic processes is significant. To reduce this energy demand, liquefied natural gas (LNG) cooling was introduced in addition to a nitrogen refrigerant to the hydrogen liquefaction process. The resultant hydrogen production from the steam methane reforming process via LNG emits carbon dioxide. Therefore, it is necessary to consider both energy and CO_2 emission when optimizing this system. To minimize these factors, single and multi-objective optimizations were performed, as well as a cost analysis in order to determine the optimal performance. The results of multi-objective optimization reveal that the CO_2 emissions decrease by 38%, whereas the total investment cost is increased by 45% compared to the base case. The specific energy consumption is increased from 10.76 kWh/kg-LH_2 to 11.13 kWh/kg-LH_2. Therefore, the compromise between the cost and the CO_2 emissions is made in the proposed case. These results will provide valuable insights regarding the economic demand and CO_2 emission for future decision-making processes.

1. Introduction

Hydrogen is a promising fossil fuel replacement as it does not contribute to pollution or produce greenhouse gases. However, hydrogen remains in the gas phase when compressed to 700 bar with low energy density of 5.6 MJ/L, making its large scale storage inefficient. Thus, the demand of liquid hydrogen has increased as a result of its high energy density (10.1 MJ/L), which gives it a higher storage capacity [1].

The primary challenge in constructing a hydrogen liquefaction plant is the high demand of energy and operating cost. The specific energy consumption (SEC) of hydrogen for current plants is in the range of 10.8–12.7 kWh/kg for the Claude cycle and 12.3–13.4 kWh/kg for the Brayton cycle [2]. Further, the price of liquid hydrogen ranged between 8 and 9 $/kg in 2017 [3]. Therefore, decreasing this energy consumption and operating cost of this process is essential.

Various researchers have performed optimizations regarding the energy and cost related to hydrogen liquefaction. Nandi et al. [4] analyzed the performance of the precooled Linde–Hampson cycle, the Claude cycle, and the helium–hydrogen condensing cycle. The Claude cycle has a guaranteed higher liquefaction efficiency compared to the Linde–Hampson cycle, whereas the helium–hydrogen condensing cycle produces 100% liquid hydrogen as a result of the helium expansion below 20 K. Bracha et al. [5] investigated a large-scale hydrogen plant with a 4.4 tonne per day (TPD) capacity located in Ingolstadt, Germany, wherein the Claude cycle was employed for hydrogen liquefaction with an ortho–para converter. Cammarata et al. [6] constructed a simple cryogenic process with the Claude cycle that is applicable to both helium or hydrogen, optimizing the energy consumption using a genetic algorithm (GA). Cardella et al. [7,8] designed a large-scale hydrogen liquefaction process with a capacity in the range of 25–100 TPD. Here, two cases with different refrigerant and liquefaction cycle were constructed and optimized in terms of the specific energy consumption and the specific liquefaction cost.

Kuendig et al. [9] developed a large-scale hydrogen liquefaction model that used liquefied natural gas (LNG) re-gasification. Similarly, Yun [10] developed a hydrogen liquefaction model with LNG as the refrigerant. Using LNG as a refrigerant is advantageous as it can achieve ~~a~~ high energy efficiency for both the hydrogen precooling and natural

* Corresponding authors.
E-mail addresses: uzahid@kfupm.edu.sa (U. Zahid), cjlee@cau.ac.kr (C.-J. Lee).

https://doi.org/10.1016/j.enconman.2021.113835
Received 29 September 2020; Accepted 6 January 2021
Available online 26 January 2021
0196-8904/

Nomenclature

W	power, kW
m	mass flow rate
T	temperature, K
h	mass enthalpy, kJ/kg
s	mass entropy, kJ/kg K
Q	heat flow, kW
x	design variables
f	fitness function
r	penalty factor
e	tolerance of energy balance error in the heat exchanger

Symbols

η	exergetic efficiency

Subscripts

LNG	liquefied natural gas
GH_2	gaseous hydrogen
N_2	nitrogen
LH_2	liquid hydrogen
CO_2	carbon dioxide
SMR	steam methane reforming
electricity	the electricity provided by the power plant
out	outlet stream
in	inlet stream
i	index

Abbreviations

LNG	liquefied natural gas
SMR	steam methane reforming
GA	genetic algorithm
SEC	specific energy consumption
LCOH	levelized cost of hydrogen
PP	payback period
CRF	capital recovery factor
CAPEX	capital expenditure
OPEX	operating expenditure

gas evaporation. However, the energy produced from evaporating the natural gas is wasted to the sea. Yang et al. [11] proposed a large-scale hydrogen liquefaction system with a capacity of 300 TPD integrated with steam methane reforming (SMR), wherein the hydrogen feed is provided by the SMR, thereby utilizing the LNG refrigerant to produce liquid hydrogen product.

Krasae-in et al. [12] developed a conceptual model involving the mixed-refrigerant precooling cycle, which can cool the hydrogen feed from 298 to 80 K, followed by ~~the~~ four-stage hydrogen Joule–Brayton cascade system, which is used for further cooling from 80 to 20 K. In addition, they also optimized the hydrogen Joule–Brayton cycle as a result of ortho–para hydrogen gas equilibrium from 80 K to 20 K [13]. Sadaghiani et al. modeled a two mixed-refrigerant precooling cycle [14]. Ansarinasab et al. [15,16] performed an exergoeconomic analysis with a model consisting of one mixed-refrigerant precooling cycle and four-stage hydrogen cryogenic cycles, wherein they analyzed the resultant exergy, exergoeconomic, and exergoenvironmental indicators to ascertain the performance of ~~the~~ hydrogen liquefaction plant. Note that a life cycle assessment was selected for the exergoenvironmental analysis. Yin et al. [17] focused on the optimization of a hydrogen liquefaction process involving liquid nitrogen precooling and helium expansion-refrigeration loop using a GA to minimize the SEC, including the performance analysis of cost and exergy. The results of the optimization were obtained, revealing energy consumption of 7.31 kWh/kg-LH_2.

Yilmaz et al. [18] introduced a coal-gasification assisted multi-generation system that included hydrogen production and liquefaction, as well as the production of heating and cooling utilities along with the power. The energy and exergy efficiencies were found to be 52.29% and 43.35%, respectively. Yuksel et al. [19] proposed a waste-to-hydrogen gasification system, wherein the gasification unit was integrated with the Brayton cycle, Stirling engine cycle, single effect absorption cooling cycle, and hydrogen production and liquefaction cycle. Notably, the production rate of hydrogen was found to be 13%.

Kanoglu et al. [20] proposed hydrogen liquefaction with the Claude cycle integrated with geothermal heat driven absorption precooling and a binary geothermal power plant. Yilmaz et al. [21] investigated the performance of this model by analyzing the energy, exergy, efficiency, and process loss. Then, optimization was performed to minimize the liquefaction cost using a GA [22]. Aasadnia et al. [23] developed a model that consists of a precooling stage with a mixed-refrigerant cycle, an absorption refrigeration cycle, and a cryogenic cooling stage with a cascade Joule–Brayton cycle. This integrated system was found to have a 6.47 kWh SEC and 45.5% efficiency.

In short, the former researches focused on improving the energy efficiency and operating cost of hydrogen liquefaction by developing refrigeration cycles with various sources of cooling energy. Some of the studies developed a hydrogen liquefaction model with LNG cooling and SMR to decrease its energy consumption and liquefaction cost. There was also an attempt to conduct an environmental analysis using life cycle assessment. However, there has been no concern of deciding optimal operating conditions satisfying economic and environmental objectives simultaneously. Since the LNG system emits carbon dioxide, it must be decreased to reduce its impact on the environment while optimizing its cost and energy. Therefore, a multi-objective optimization regarding economic and environmental factors must be performed for the LNG-integrated hydrogen liquefaction process system. In this study, the hydrogen liquefaction model with LNG system is adapted as a base case, then single and multi-objective optimization of energy, cost and CO2 emissions are performed to discover its performance using a genetic algorithm. In addition, a decision-making is suggested in order to select one operating condition from multiple optimal options.

2. Materials and methods

2.1. Process modeling

The process model is constructed using Aspen HYSYS V10 based on the hydrogen liquefaction system proposed by Yang et al. [11]. The process flow diagram is shown in Fig. 1.

This system differs from the previous model as the Brayton cycle of the nitrogen and hydrogen stream herein are simplified, resulting in one refrigeration cycle for each stream, thereby reducing the number of expanders. Since the purpose of the previous study was to replace the N_2 refrigerant to LNG, the structure of the N_2 cycle have been modified.

First, the gaseous hydrogen feed (GH_2) enters the cooling system (GH_2-1). The hydrogen feed is the summation of the production from steam methane reforming (SMR) and the hydrogen make-up to maintain the product capacity as 300 TPD. This feed is precooled from the plate fin type heat exchangers (HX-1, HX-2, and HX-3). The refrigerants used in this system are liquid nitrogen (N_2-1), liquefied natural gas (LNG-1), and the hydrogen Brayton cycle (GH_2-4). Their flowrates are 50 TPD, 931 TPD and 246 TPD respectively. The temperature profiles of these heat exchangers are modified from a previous work in order to satisfy

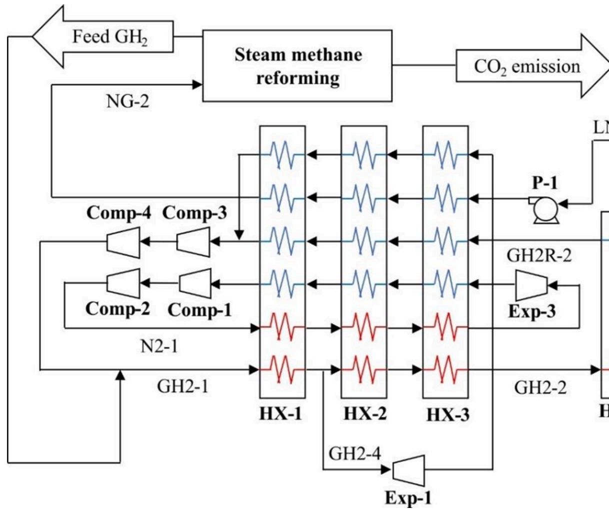

Fig. 1. Process flow diagram of the hydrogen liquefaction system modified from previous research [11].

the thermodynamic properties of each stream, including equilibrium hydrogen. The heat composite curve data for the heat exchangers are shown in Fig. 2. In HX-2, the cold composite curve shows nonlinear behavior due to the phase change of LNG refrigerant. In HX-3, however, the cold composite shows the linear correlation due to the small amount of N_2 refrigerant. When the flowrate of N_2 refrigerant increases, the influence of the phase change of N_2 is applied to the curve. After the precooling section, the precooled temperature (GH_2-2) reaches approximately 100 K, which is achieved through the use of LNG refrigerant and hydrogen Brayton cycle. The feed is further cooled by the passing through heat exchangers (HX-4 and HX-5). After the expansion, liquid hydrogen is produced. The vapor phase hydrogen ~~flow~~ which is not liquefied in vessel (S-1) is recycled back to the process. The separated flow of hydrogen (GH_2-4) provides additional power to the electric and cooling energy via the Brayton cycle. The LNG-1 enters the SMR system after the cooling process, producing carbon dioxide and hydrogen.

2.2. Operating conditions

The specifications of the process are summarized in Table 1. Note that most of the parameters are adapted from the previous research [11]. Herein, the liquefaction rate is assumed to be 12% [4]. The purity of the liquid hydrogen product is assumed as 100%. The minimum

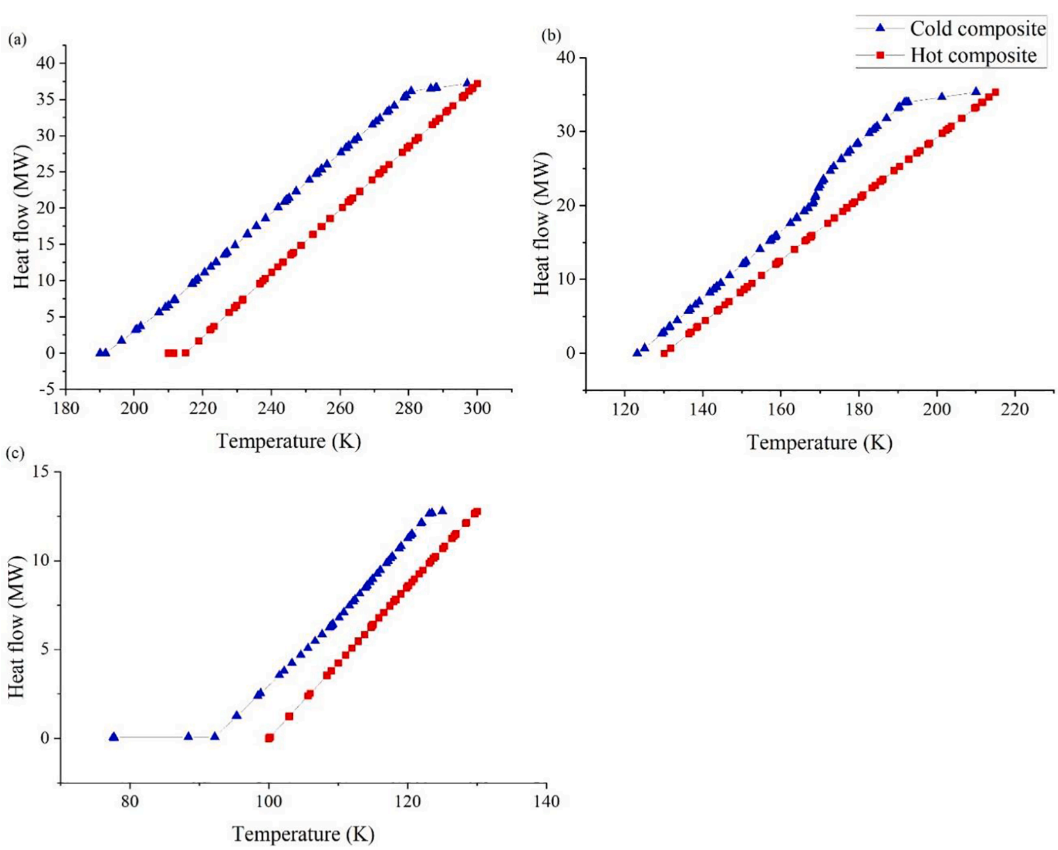

Fig. 2. Heat composite curve with respect to temperature and heat flow for the heat exchangers (HX) (a) HX-1, (b) HX-2, and (c) HX-3.

Table 1
Specifications of liquefaction system.

Parameter	Value
Feed condition	
Feed pressure	20 bar
Feed temperature	300 K
Product condition	
Product capacity	300 tonne per day
Product pressure	1.3 bar
Product temperature	20.38 K
Liquefaction rate	12%
Purity	100%
Mechanical efficiency	
Isentropic efficiency of compressor	80%
Isentropic efficiency of expander	90%
Adiabatic efficiency of pump	75%
Heat exchanger	
Minimum temperature approach	1–10 K
Ortho–para conversion	Continuous

temperature approach of each heat exchanger ranges between 1 and 10 K. The Peng–Robinson equation of state is used to determine the thermodynamic properties of the overall process, wherein the ortho–para conversion of hydrogen is assumed to be continuous and its thermodynamic properties are adapted from the literature [24].

3. Optimization method

A genetic algorithm (GA) is selected for single and multi-objective optimizations. GA has been widely used in process design because of the simplicity and the stochastic properties which are able to handle the process with complicated systems such as non-linear equations and thermodynamics [25]. The optimization procedure is illustrated in Fig. 3. When the algorithm starts within MATLAB, the population embedded in the design variables is initialized. The design variable configured by the GA is exported to the process model programmed in Aspen HYSYS. The model data calculated are then imported to MATLAB. If the data do not satisfy the constraints, a penalty function is directly added to the fitness function. Otherwise, the fitness function is obtained based on the data, some of which are exported to Microsoft Excel or the economic analysis. The algorithm repeats during selection, crossover, or mutation to create a new population until the fitness value meets the tolerance. The parameters of the GA options are listed in Table 2.

3.1. Configurations for optimization

As the motivation of this optimization is to minimize energy demand, operating cost, and carbon dioxide emissions, certain design variables and objective functions are adopted to satisfy these purposes.

The parameters of the base case are configured based on the proposed model from the previous work [11]. The design variables of the process are the flow rates of the refrigerants. Their ranges are as follows:

$$\begin{aligned} x &= [m_{LNG}, m_{GH_2-4}, m_{N_2}], \\ m_{LNG} &\leq 931.2, (\mathrm{TPD}) \\ m_{GH_2-4} &\leq 600, (\mathrm{TPD}) \\ m_{N_2} &\leq 1000(\mathrm{TPD}). \end{aligned} \quad (1)$$

The upper bound of the LNG flow rate is derived from the production of 300 TPD of the hydrogen feed, as provided by SMR. Since the product capacity of liquid hydrogen is 300 TPD, the hydrogen from SMR and the

Table 2
Parameters of genetic algorithm options used for both single and multi-objective optimizations.

Parameter	Value
Population size	300
Crossover fraction	80%
Selection function	Tournament
Tournament size	4
Mutation function	Adapt feasible

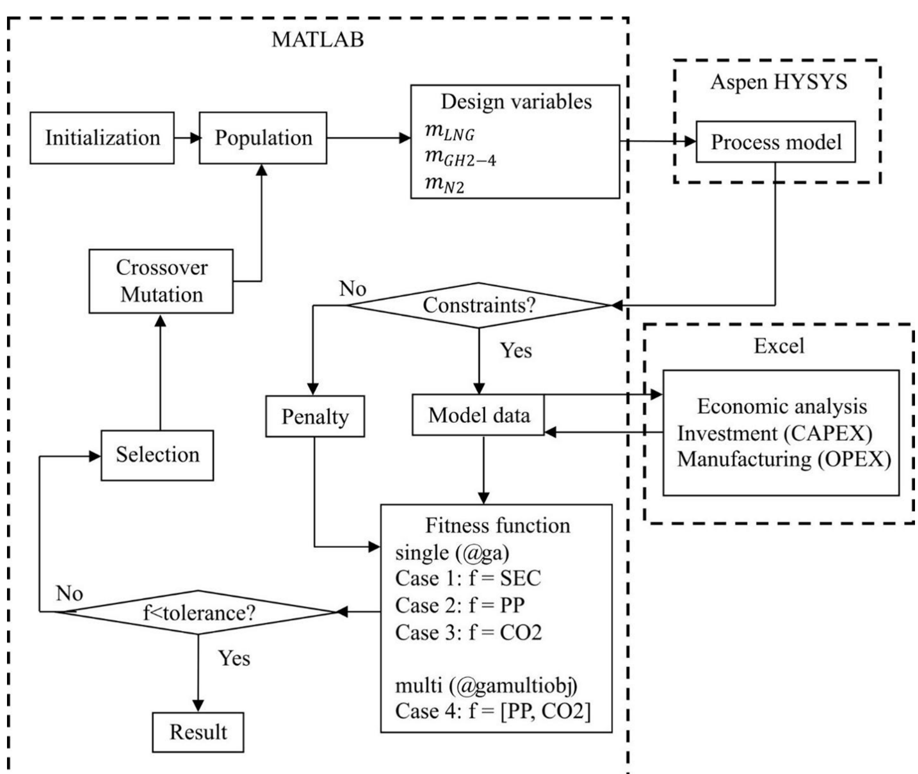

Fig. 3. Procedure framework to perform optimization with process model data and economic analysis.

hydrogen make-up are added to maintain the mass balance. If the LNG flowrate is lower than 931.2 TPD, then hydrogen make-up is applied to the hydrogen feed to maintain 300 TPD. The lower bounds of all variables are set as zero. The other conditions are set to arbitrary values that are sufficient for providing cold energy in the heat exchangers.

Constraints with respect to the energy balance of heat exchangers are also added to converge the model. As the design variables are arbitrary due to the stochastic nature of the GA, the energy balance of the heat exchangers does not converge in the specific cases. Therefore, to exclude these scenarios, the penalty function is adopted and multiplied by a penalty factor [26]. Any deviation from the energy balance can be found by adding the enthalpy of all the streams through the heat exchanger [27]. If its resultant value exceeds the error tolerance, the penalty function substitutes the fitness function.

$$Q = m(h_{in} - h_{out}), \quad if|Q| \geq e, \quad minimize\ f = r^*|Q| \tag{2}$$

3.1.1. Specific energy consumption

The SEC is defined as the summation of power consumption of the compressors and expanders per unit mass of the product [25]. Note that the unit of the SEC is kWh/kg-LH_2.

$$SEC = \frac{W}{m_{LH_2}} = \frac{\sum W_{comp} - \sum W_{exp}}{m_{LH_2}} \tag{3}$$

The exergetic efficiency must also be calculated for the detailed analysis of the results. The definition of the exergetic efficiency is the ratio between the exergy of the product and the work [25].

$$\eta = \frac{(h_{out} - h_{in}) - T_0(s_{out} - s_{in})}{W} \tag{4}$$

3.1.2. Economic analysis

The parameters and equations of the cost estimation are based on the literature [28,29]. The objective functions for the economic analysis consider a payback period (PP), which is defined as:

$$Payback\ period = \frac{Initial\ investment}{Annual\ cash\ flow} \tag{5}$$

The levelized cost of hydrogen (LCOH) is also considered to evaluate the results [30]. The definition of the LCOH is the annual expenditure of unit mass product. In other words, it is an estimation of the price of the product. The annual cost can be found by the summation of the annual investment and manufacturing cost. Meanwhile, the capital recovery factor (CRF) is the conversion of the annual interest rate to that of the plant lifetime.

$$LCOH = \frac{Investment \times CRF + Manufacturing}{m_{LH_2}} \tag{6}$$

Detailed information regarding the economic analysis can be found in Turton and Douglas [28,29].

3.1.3. CO_2 emission

CO_2 emissions are the result of the integration of the SMR process emissions and the power plant that produces the electricity. The source of the power plant and CO_2 emissions per unit electricity are derived from the Organization for Economic Cooperation and Development (OECD) report [31].

$$CO_2\ emission = CO_2\ from\ SMR + CO_2\ from\ electricity \tag{7}$$

3.2. Single-objective optimization

A single-objective optimization is performed using a GA, wherein the objective functions are selected as energy, cost, and the environment. The objective functions, which include SEC, PP, and CO_2 emissions, are allocated to cases 1, 2, and 3, respectively.

$$Case1: minimize\ f = SEC = \frac{W}{m_{LH_2}} \tag{8}$$

$$Case2: minimize\ f = PP \tag{9}$$

$$Case3: minimize\ f = m_{CO_2} = m_{CO_2,SMR} + m_{CO_2,electricity} \tag{10}$$

3.3. Multi-objective optimization

Because the cost and environmental functions have a tradeoff relationship, a multi-objective GA is performed to compromise these aspects. Unlike single-objective GA, multi-objective optimization involves more than one objective function with multi-dimensional space. In other words, objective vectors are considered during optimization. When optimizing two objective functions, the results are shown on the 2-dimensional space called pareto optimal front [32]. The objective functions for this case (case 4) are the PP and CO_2 emissions.

$$Case4: minimize\ f_1 = PP, \quad minimize\ f_2 = m_{CO_2} \tag{11}$$

4. Results and discussion

4.1. Single-objective optimization

The optimization results of cases 1, 2, and 3 are listed in Table 3. The results of the fitness function by a single GA are shown in Fig. 4. The cost breakdown of capital expenditure (CAPEX) and operating expenditure (OPEX) is described in Fig. 6. In comparison with the base case, cases 1 and 2 are both energy and cost effective, whereas case 3 has both high energy demand and cost. For cases 1 and 2, the LNG flow rate maintains its maximum, which is consistent with the base case, while the flow rates of GH_2 and N_2 decrease. This is the result of the duty of hydrogen compressors, which are influenced by the flow rate of the hydrogen steam, having a large impact on the total energy demand as shown in Table 4. In case 3, however, the LNG flow rate is the lowest as most of the CO_2 emissions are produced from the SMR process. The flow rates of GH_2 and N_2 contribute the cold energy in the heat exchangers. From the economic analysis, both CAPEX and OPEX are the lowest in case 1 and 2, and the highest in case 3. The CAPEX mainly depends on the hydrogen compressor, while the OPEX is mostly affected by the material costs of hydrogen, nitrogen and LNG. In conclusion, the maximum usage of LNG refrigerant to produce hydrogen feed without make-up and the minimum flowrates of hydrogen and nitrogen cycles become the most

Table 3
Summary of results for multi-objective optimization for each case.

Parameter	Unit	Base case	Case 1	Case 2	Case 3	Case 4
Feed condition	**Tonne per day (TPD)**					
Liquified natural gas		931	921	931	26	371
GH_2		246	50	51	453	261
N_2		50	8	10	33	7
Energy efficiency						
Specific energy consumption	kWh/kg-LH_2	10.76	10.26	10.26	11.83	11.13
Efficiency	%	36.76	40.08	40.03	35.73	37.90
Economic analysis						
Levelized cost of hydrogen	\$/kg-LH_2	3.10	2.99	2.97	5.46	4.50
Payback period	Yr	5.43	5.18	5.15	13.41	8.40
Environment	**TPD**					
CO_2 emissions		3911	3819	3845	1596	2441

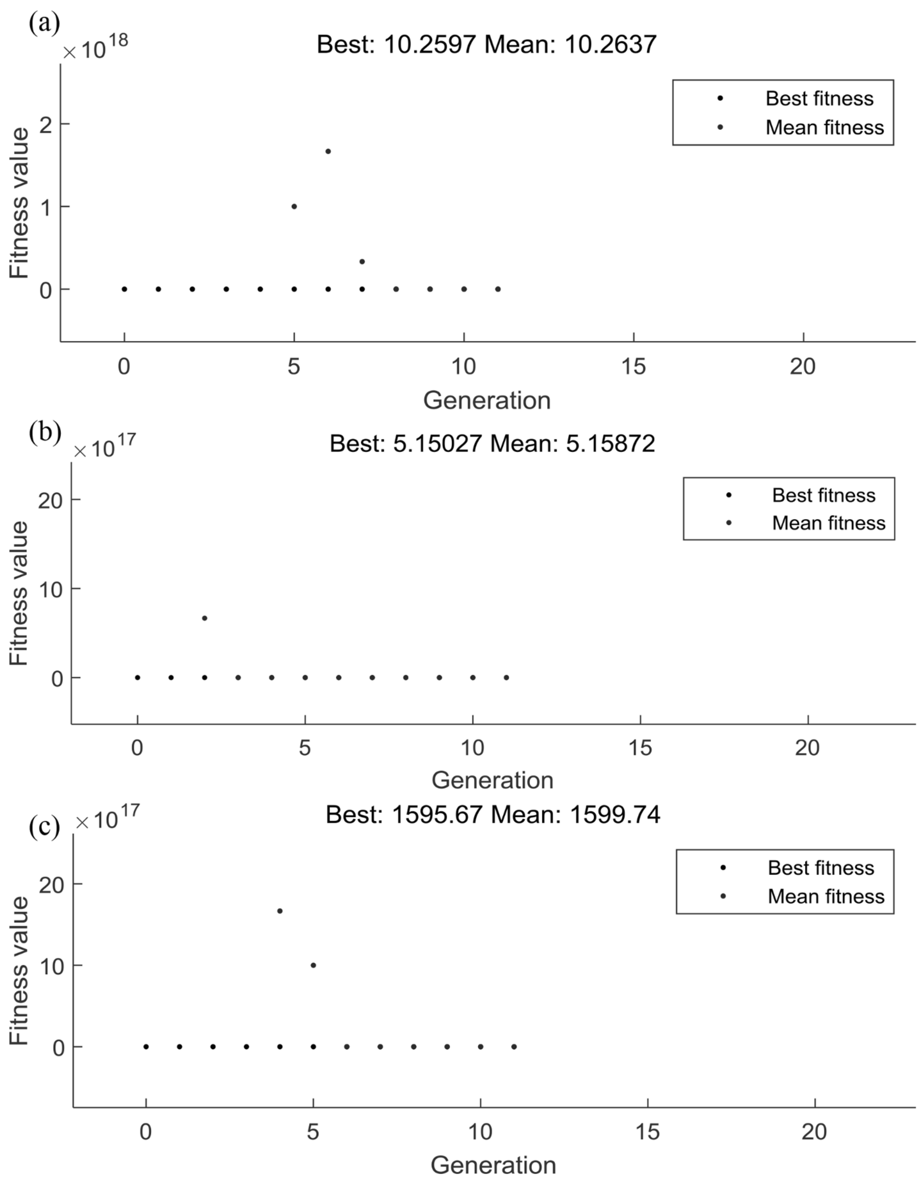

Fig. 4. The results of single genetic algorithms for cases (a) 1, (b) 2, and (c) 3.

Table 4
Power consumption of the compressor and expander in the multi-objective optimization results.

Parameter	Unit	Base case	Case 1	Case 2	Case 3	Case 4
Compressor	**kW**					
N_2 compressor		252	39	49	166	34
H_2 compressor		146,762	137,309	137,283	163,895	151,848
Expander	**kW**					
Expander		12,763	9329	9347	16,385	13,017

efficient in terms of economic objective.

4.2. Multi-objective optimization

The results of the multi-objective optimization appear as the pareto-optimal frontier, as shown in Fig. 5.

The correlation between CO_2 emission and cost reveals a tradeoff relationship. Thus, if the cost is optimized, then the maximum emission

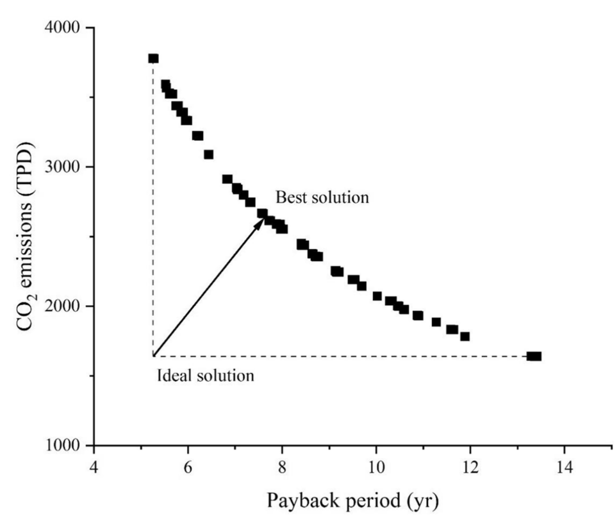

Fig. 5. Pareto-optimal frontier of the multi-objective genetic algorithm.

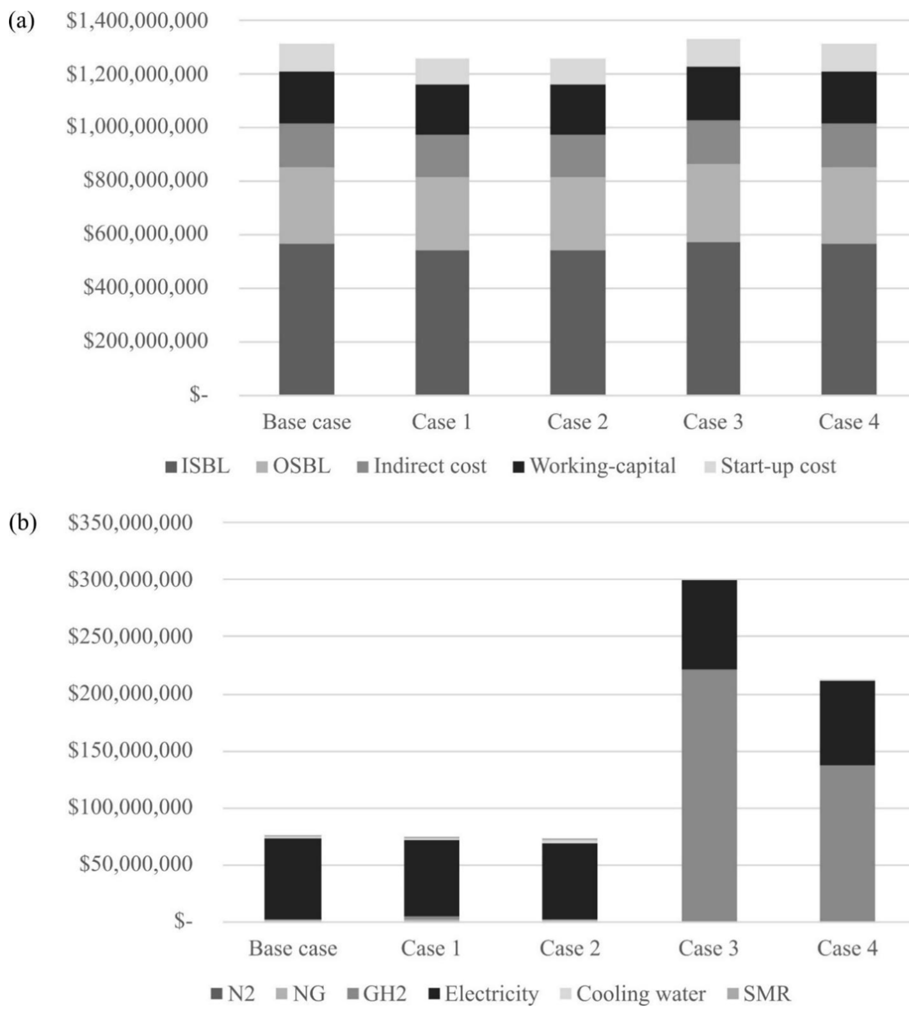

Fig. 6. The cost breakdown of capital expenditure (CAPEX) and operating expenditure (OPEX).

of the greenhouse gases is inevitable. Conversely, if the CO_2 emissions are decreased, there is an additional cost.

Due to the nature of the pareto frontier, every result is an optimal point. There are several standards to decide which should be selected. The common method to identify the best solution is to calculate the distance between the ideal solution, which satisfies minimization of both objective functions, and pareto frontier. The pareto front is normalized before calculating the distance, then the best solution is

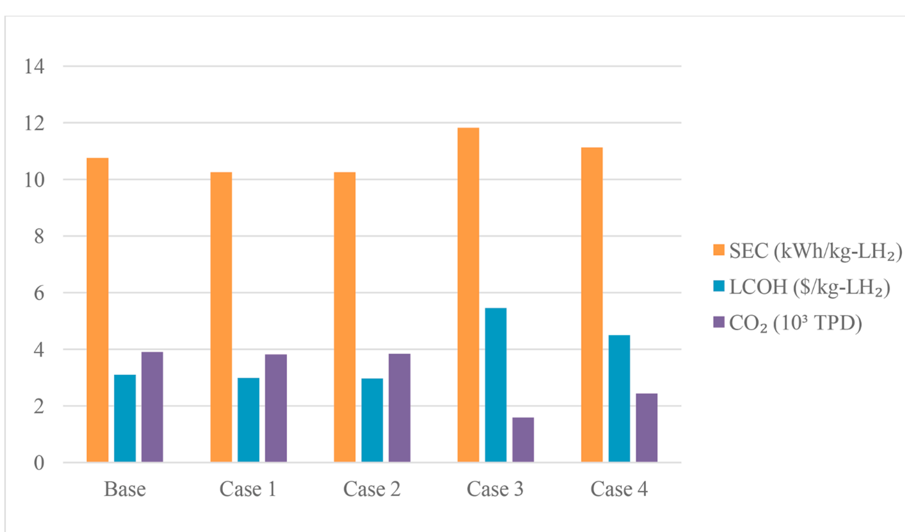

Fig. 7. Comparison between cases of (a) specific energy consumption (SEC) (kWh/kg-LH_2), (b) levelized cost of hydrogen (LCOH) ($/kg-$LH_2$), and (c) CO_2 emission (TPD).

selected as the closest point to the ideal solution. This solution is set as a case 4. The details of this procedure have been explained by Sayyaadi [33].

As a result, the optimal point of the optimization is found to be 371 TPD of LNG, 261 TPD of GH_2-4, and 7 TPD of N_2 with 2441 TPD of CO_2 emissions. This is the optimal compromise between the cost and environment aspects.

In the compromised case, the LCOH is higher than the base case, showing an increase of approximately 45%. On the other hand, the CO_2 emissions decreased by approximately 38%. Further, the LNG flow rate decreased 60% compared to that of the base case, while the flow rate of GH_2 increased to compensate for the reduced flow rate of the LNG refrigerant. The N_2 flow rate remains low because it affects the N_2 compressor, which increases the energy consumption. The economic analysis with the cost breakdown shows that the hydrogen material cost increases in OPEX, because the hydrogen make-up is applied to supplement the hydrogen feed from LNG. The CAPEX also increases due to the power consumption of the compressors.

The overall tendencies of the cases are shown in Fig. 7. Both the energy consumption and the cost decrease in cases 1 and 2, and while showed an increasing trend for the case 3. However, the CO_2 emissions showed an opposite trend, that is increase in emissions for case 1 and case 2, while a reduction in case 3 compared to the base case design. The compromise of these cases is made in case 4. The CO_2 emissions of case 4 is higher than case 3, and lower than cases 1 and 2. On the other hand, the SEC and the payback period of case 4 decrease compared to case 3, but both objectives are higher than those of cases 1 and 2.

These correlations show that the introduction of LNG cooling with the SMR process is the most dominant factor in improving both the cost and environmental objectives. The decreased demand on the compressors is the result of the decreased mass flow rates of H_2 and N_2 streams, which lead to a decrease in both energy consumption and operating cost. At the same time, an increase in the CO_2 emission in the SMR process is caused from the LNG flow. Therefore, a compromise between the cost and environmental results is conducted based on the multi-objective optimization. The best solution of the multi-objective optimization which is the closest to the ideal point shows a decrease of CO_2 emissions by 38% and an increase of capital and operating cost by 45%. A further decision-making is possible based on this quantitative standard by considering whether one objective is more important than the other.

5. Conclusions

Optimization of the hydrogen liquefaction process integrated with SMR was conducted to reduce its cost and environmental impacts. Herein, a base case was established from the proposed model based on previous research. Single-objective optimizations were performed for SEC, PP, and CO_2 emissions in order to obtain an optimal solution for each case. Further, a multi-objective optimization of the PP and CO_2 emissions was performed to identify the optimal point of the performance. The results reveal that the maximum usage of LNG and minimum flow rates of GH_2 and N_2 guarantee energy and cost efficiency, while the CO_2 emissions increase substantially. These results also indicate that even if the economic cost increases by 45% in comparison with the base case, total CO_2 emissions decrease by 38%. The SEC of the compromised case experiences an energy requirement increase from 10.76 kWh/kg-LH_2 to 11.13 kWh/kg-LH_2. These results provide a quantitative standard when proceeding the future decision-making processes regarding the economic demand and CO_2 emissions. In other words, advanced decision-making such as modifying the process to give an importance to one objective will be possible based on the concept of best solution. The limitation of the study, however, is that the process model has intrinsically high demand of energy consumption. The future study will be the modification of the model to reduce the energy demand and further optimization with consideration of energy, economic or environmental objectives.

CRediT authorship contribution statement

Ju-Eon Bae: Writing - original draft, Conceptualization, Methodology. **Supaporn Wilailak:** Validation, Investigation. **Jae-Hyeon Yang:** Resources, Conceptualization. **Dong-Yeol Yun:** Data curation, Software. **Umer Zahid:** Writing - review & editing. **Chul-Jin Lee:** Supervision.

Declaration of Competing Interest

The authors declare that they have no known competing financial interests or personal relationships that could have appeared to influence the work reported in this paper.

Acknowledgements

This research was supported by a grant(20IHTP-B151617-02) from Development of Core Technologies for Commercial Hydrogen Liquefaction Plant Program funded by Ministry of Land, Infrastructure and Transport of Korean government and the Chung-Ang University Graduate Research Scholarship in 2020.

References

[1] Mazloomi K, Gomes C. Hydrogen as an energy carrier: Prospects and challenges. Renew Sustain Energy Rev 2012;16:3024–33. https://doi.org/10.1016/j.rser.2012.02.028.
[2] Ohlig K, Decker L. The Latest Developments and Outlook for Hydrogen Liquefaction Technology. AIP Conf Proc 2013;1573. https://doi.org/10.1063/1.4860858.
[3] Reddi K, Elgowainy A, Rustagi N, Gupta E. Impact of hydrogen refueling configurations and market parameters on the refueling cost of hydrogen. Int J Hydrogen Energy 2017;42:21855–65. https://doi.org/10.1016/j.ijhydene.2017.05.122.
[4] Nandi TK, Sarangi S. Performance and optimization of hydrogen liquefaction cycles. Int J Hydrogen Energy 1993;18:131–9. https://doi.org/10.1016/0360-3199(93)90199-K.
[5] Bracha M, Lorenz G, Patzelt A, Wanner M. Large-scale hydrogen liquefaction in Germany. Int J Hydrogen Energy 1994;19:53–9. https://doi.org/10.1016/0360-3199(94)90177-5.
[6] Cammarata G, Fichera A, Guglielmino D. Optimization of a liquefaction plant using genetic algorithms. Appl Energy 2001;68:19–29. https://doi.org/10.1016/S0306-2619(00)00041-6.
[7] Cardella U, Decker L, Sundberg J, Klein H. Process optimization for large-scale hydrogen liquefaction. Int J Hydrogen Energy 2017;42:12339–54. https://doi.org/10.1016/j.ijhydene.2017.03.167.
[8] Cardella U, Decker L, Klein H. Economically viable large-scale hydrogen liquefaction. IOP Conf Series Mater Sci Eng 2017;171:012013. https://doi.org/10.1088/1757-899X/171/1/012013.
[9] Kuendig A, Loehlein K, Kramer GJ, Huijsmans J. Large scale hydrogen liquefaction in combination with LNG re-gasification. In: 16th World Hydrogen Energy Conference 2006; 2006. p. 3326–33.
[10] Yun S-K. Design and Analysis for Hydrogen Liquefaction Process Using LNG Cold Energy. J Korean Inst Gas 2011;15. https://doi.org/10.7842/kigas.2011.15.3.001.
[11] Yang J-H, Yoon Y, Ryu M, An S-K, Shin J, Lee C-J. Integrated hydrogen liquefaction process with steam methane reforming by using liquefied natural gas cooling system. Appl Energy 2019;255:113840. https://doi.org/10.1016/j.apenergy.2019.113840.
[12] Krasae-in S, Stang JH, Neksa P. Simulation on a proposed large-scale liquid hydrogen plant using a multi-component refrigerant refrigeration system. Int J Hydrogen Energy 2010;35:12531–44. https://doi.org/10.1016/j.ijhydene.2010.08.062.
[13] Krasae-in S. Optimal operation of a large-scale liquid hydrogen plant utilizing mixed fluid refrigeration system. Int J Hydrogen Energy 2014;39:7015–29. https://doi.org/10.1016/j.ijhydene.2014.02.046.
[14] Sadaghiani MS, Mehrpooya M. Introducing and energy analysis of a novel cryogenic hydrogen liquefaction process configuration. Int J Hydrogen Energy 2017;42:6033–50. https://doi.org/10.1016/j.ijhydene.2017.01.136.
[15] Ansarinasab H, Mehrpooya M, Mohammadi A. Advanced exergy and exergoeconomic analyses of a hydrogen liquefaction plant equipped with mixed refrigerant system. J Cleaner Prod 2017;144:248–59. https://doi.org/10.1016/j.jclepro.2017.01.014.
[16] Ansarinasab H, Mehrpooya M, Sadeghzadeh M. An exergy-based investigation on hydrogen liquefaction plant-exergy, exergoeconomic, and exergoenvironmental analyses. J Cleaner Prod 2019;210:530–41. https://doi.org/10.1016/j.jclepro.2018.11.090.
[17] Yin L, Ju Y. Process optimization and analysis of a novel hydrogen liquefaction cycle. Int J Refrig 2020;110:219–30. https://doi.org/10.1016/j.ijrefrig.2019.11.004.

[18] Yilmaz F, Ozturk M, Selbas R. Design and thermodynamic analysis of coal-gasification assisted multigeneration system with hydrogen production and liquefaction. Energy Convers Manage 2019;186:229–40. https://doi.org/10.1016/j.enconman.2019.02.053.
[19] Yuksel YE, Ozturk M, Dincer I. Energy and exergy analyses of an integrated system using waste material gasification for hydrogen production and liquefaction. Energy Convers Manage 2019;185:718–29. https://doi.org/10.1016/j.enconman.2019.02.033.
[20] Kanoglu M, Yilmaz C, Abusoglu A. Geothermal energy use in absorption precooling for Claude hydrogen liquefaction cycle. Int J Hydrogen Energy 2016;41:11185–200. https://doi.org/10.1016/j.ijhydene.2016.04.068.
[21] Yilmaz C, Kaska O. Performance analysis and optimization of a hydrogen liquefaction system assisted by geothermal absorption precooling refrigeration cycle. Int J Hydrogen Energy 2018;43:20203–13. https://doi.org/10.1016/j.ijhydene.2018.08.019.
[22] Yilmaz C. A case study: Exergoeconomic analysis and genetic algorithm optimization of performance of a hydrogen liquefaction cycle assisted by geothermal absorption precooling cycle. Renew Energy 2018;128:68–80. https://doi.org/10.1016/j.renene.2018.05.063.
[23] Aasadnia M, Mehrpooya M. Conceptual design and analysis of a novel process for hydrogen liquefaction assisted by absorption precooling system. J Cleaner Prod 2018;205:565–88. https://doi.org/10.1016/j.jclepro.2018.09.001.
[24] Eckroll J. Concepts for Large Scale Hydrogen Liquefaction Plants. Norwegian University of Science and Technology Department of Energy and Process Engineering; 2017.
[25] Yin L, Ju YL. Comparison and analysis of two nitrogen expansion cycles for BOG Re-liquefaction systems for small LNG ships. Energy 2019;172:769–76. https://doi.org/10.1016/j.energy.2019.02.038.
[26] Song R, Cui M, Liu J. Single and multiple objective optimization of a natural gas liquefaction process. Energy 2017;124:19–28. https://doi.org/10.1016/j.energy.2017.02.073.
[27] Watson HAJ, Khan KA, Barton PI. Multistream heat exchanger modeling and design. AIChE J 2015;61:3390–403. https://doi.org/10.1002/aic.14965.
[28] Turton R. Analysis, Synthesis, and Design of Chemical Processes. Prentice Hall; 2012.
[29] Douglas JM, Douglas M. Conceptual Design of Chemical Processes. McGraw-Hill; 1988.
[30] Viktorsson L, Heinonen JT, Skulason JB, Unnthorsson R. A Step towards the Hydrogen Economy—A Life Cycle Cost Analysis of A Hydrogen Refueling Station. Energies 2017;10:763.
[31] Carbon Pricing, Power Markets and the Competitiveness of Nuclear Power. OECD Publishing 2011.
[32] Amouzgar K. Multi-objective optimization using Genetic Algorithms. Jönköping University School of Engineering; 2012.
[33] Sayyaadi H, Babaelahi M. Multi-objective optimization of a joule cycle for re-liquefaction of the Liquefied Natural Gas. Appl Energy 2011;88:3012–21. https://doi.org/10.1016/j.apenergy.2011.03.041.